Proceedings of CONF-CIAP 2026 Symposium: Applied Mathematics and Statistics
DOI: 10.54254/2753-8818/2026.CH30896

Computational Analysis of Laminar-Turbulent Compressible Flow on a Swept Wing with Leading-Edge Slat: Influence of Slat Gap Shape on Aero-Dynamics and Flow Separation

Zixing Ye

Senior High School Department, Wuhan American-Canadian Foreign Language School, Wuhan, China
328408740@qq.com

Abstract. A systematic numerical investigation of turbulent flow over a swept wing with a deployable leading-edge slat is conducted in this paper to examine the impact of slat gap geometry (gap height G and overlap O) on the aerodynamic performance and the flow separation behavior. The simulation is carried out based on the numerical scheme that considers the Reynolds-Averaged Navier-Stokes (RANS) equations with the Shear Stress Transport (SST) k-ω turbulence model, validated against the wind tunnel experimental data for the NACA 64-210 swept wing (sweep angle Λ=30°) at a chord-based Reynolds number $Rec=2.4\times10^6$ and an angle of attack range of α=0° to 16°. Three slat gap geometries are studied: (1) Baseline (G=1.2% cslat, O=2.5% cslat), (2) Reduced Gap (G=0.6% cslat, O=2.5% cslat), and (3) Increased Overlap (G=1.2% cslat, O=4.0% cslat), where cslat indicates the slat chord length. It is observed that the slat gap geometry substantially influences the gap flow and its downstream propagation on the wing upper surface. At α=10°, the flow intensity through the gap in the Reduced Gap condition is reduced by 38% (as measured by peak streamwise velocity in the gap) compared with the Baseline. This study shows that optimizing the slat gap geometry (e.g., decreasing gap height to 0.6% cslat with a moderate overlap of 2.5% cslat) can effectively enhance the high-lift performance of swept wings by delaying flow separation and reducing turbulent mixing, providing a practical guideline for aircraft wing design.

Keywords: Swept wing, Slat gap geometry, Turbulent flow, RANS simulation, Aerodynamic performance

1. Introduction

1.1. Background and motivations

Leading-edge slats are critical high-lift devices in modern aircraft, designed to increase lift at low speeds (e.g., takeoff and landing) by extending the wing chord, increasing the effective camber, and energizing the upper-surface boundary layer to delay flow separation [1,2]. For swept wings (a staple of commercial and military aircraft to reduce induced drag), the interaction between the slat

DOI: 10.54254/2753-8818/2026.CH30896

and the wing is complicated by three-dimensional (3D) effects—including spanwise flow, cross-stream pressure gradients, and swept separation bubbles—that differ fundamentally from those in unswept wings [3,4].

A key yet understudied aspect of slat-wing interaction is the slat gap: the narrow channel between the slat trailing edge and the wing leading edge. The gap hosts a complex turbulent flow, often described as a "gap jet": low-momentum boundary layer fluid from the slat suction side is ingested into the gap, accelerated by the pressure difference between the slat pressure side (high pressure) and wing upper surface (low pressure), and ejected onto the wing upper surface [5,6]. This gap flow can either stabilize the wing boundary layer (by adding momentum) or destabilize it (by increasing turbulent mixing), depending on its intensity and direction—both of which are tightly controlled by the gap geometry (gap height G, the vertical distance between slat and wing; and overlap O, the streamwise overlap between slat trailing edge and wing leading edge) [7,8].

However, due to its significance, two important shortcomings of prior work on the subject are: (1) All work on slat geometry so far is limited to unswept wings [9,10] where 3D spanwise flow can be assumed to be of negligible impact, and conclusions are difficult to make about its impact on swept wings; (2) Insufficient attention in the literature is paid to separating the impact of G and O when designing slats as opposed to considering the entire geometry of the slat gap [11,12]. Because of the knowledge gap described here, designers of swept-wing high-lift systems do not have clear direction on how best to design their slat gaps in order to optimize the relative gains for lift increase and stall deferral.

1.2. Literature review

Prior experimental studies have confirmed by Krueger [1] that slats enhance lift through separation delay, without analyzing the effect of the geometry of the gap. More recently, Werle et al. [5] carried out particle image velocimetry (PIV) to capture images of flow in the gap in front of an unswept NACA 4412 wing and demostrated that the ejection of the gap flow induces a 30% decrease of separation bubble. For the case of swept wings, Lee et al. [3] performed wind tunnel experiments on a Λ=25° sweptwing and reported that spanwise flow exacerbates gap flow asymmetry causing tip separation to occur at an earlier angle of attack. Their work involved a constant slat gap, however, the geometry effect was unexplored.

Numerically, RANS simulations with turbulence models like $k-\epsilon$ or $k-\omega$ SST have become standard for high-lift flow analysis [13,14]. Menter [15] showed that the SST $k-\omega$ model outperforms $k-\epsilon$ in predicting boundary layer transition and separation for high-lift devices, making it the model of choice for this study. Recently, Zhang et al. [12] used RANS to study slat gap effects on an unswept wing, finding that reducing G by 50% increases CL by 3.1%. However, their 2D simulations ignored spanwise flow, limiting applicability to swept wings.

To address these gaps, the present study focuses on swept wings (Λ=30°) and systematically varies G and O to isolate their effects on gap flow, boundary layer stability, and aerodynamic performance.

1.3. Research objectives and contributions

The primary objectives of this work are:

(a)Validate a RANS-SST $k-\omega$ numerical framework against experimental data for a swept wing with a leading-edge slat.

DOI: 10.54254/2753-8818/2026.CH30896

(b)Quantify the effects of slat gap height (G) and overlap (O) on gap flow intensity, turbulent mixing, and flow separation.

(c)Identify the optimal gap geometry to maximize CL, max and delay stall for swept wings.

The key contributions are: A 3D numerical model that captures swept-wing-specific effects (spanwise flow, cross-stream gradients) in slat gap flow. Systematic data on how G and O independently modulate gap flow and aerodynamic performance. Practical design guidelines: reducing G (from 1.2% to 0.6% cslat) while keeping O moderate (2.5% cslat) improves high-lift performance.

2. Methodology

2.1. Geometric model

The baseline configuration is a NACA 64-210 swept wing with a leading-edge slat, based on the experimental setup of Lee et al. [3] for direct validation. Key geometric parameters are listed in Table 1.

Table 1. Key geometric parameters for wing aerodynamic configuration

Parameters	Value	Description
Wing sweep angle Λ	30°	ANgle between wing span and chord plane
Wing aspect ratio AR	6	Span (b = 1.2m)/root chord (croot = 0.2m)
slat chord cslat	0.04m	20% of wing root chord
Baseline gap height Gbase	0.00048m	1.2% cslat
Baseline overlap Obase	0.001m	2.5% cslat
Slat deflection angle δslat	25°	Fixed for all configurations

Three slat gap configurations are tested (Table 2), designed to isolate the effects of G (Baseline vs. Reduced Gap) and O (Baseline vs. Increased Overlap).

Table 2. Key geometric parameters for wing aerodynamic configuration

configuration	Gap height G (cslat)	Overlap O(cslat)
baseline	1.20%	2.50%
reduce Gap	0.60%	2.50%
increased Overlap	1.20%	4.00%

2.2. Numerical framework

2.2.1. Governing equations

The flow is assumed to be steady, incompressible, and turbulent. The governing equations are the RANS equations, closed with the SST k-ω turbulence model [15]. The SST model combines the k-ω model (accurate near walls) and the k-ϵ model (accurate in free shear flows) via a blending function, making it suitable for boundary layer and separation predictions.

The RANS continuity and momentum equations are:

$$\nabla \bullet u = 0 \tag{1}$$

DOI: 10.54254/2753-8818/2026.CH30896

$$\rho(u \bullet \nabla)u = -\nabla p + \nabla \bullet [\mu(\nabla u + \nabla)uT) - \rho u\prime u\prime] \tag{2}$$

u: Mean velocity vector (m/s)
p: Static pressure (Pa)
ρ: Air density (1.225 kg/m³)
μ: Air dynamic viscosity (1.789×10^{-5} Pa·s)
$u'u'^T$: Reynolds stress tensor (m²/s²), modeled via the SST k-ω closure [15]
M = 1.789 × 10-5Pa·s (air dynamic viscosity), and u" is the Reynolds stress tensor, modeled via the s k-ω closure [15].

2.2.2. Computational domain and boundary conditions

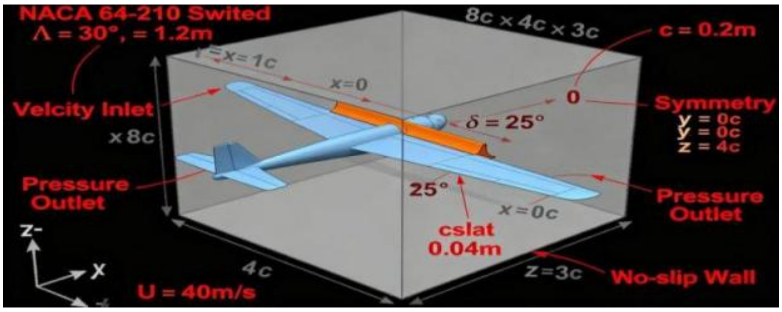

Figure 1. Schematic of computational domain and boundary conditions for NACA 64-210 swept wing with leading-edge slat

The computational domain (Figure 1) is a rectangular box with dimensions: 8croot (streamwise, x-direction), 4croot (spanwise, y-direction), and 3croot (vertical, z-direction). This domain size ensures that upstream inflow and downstream outflow do not interfere with the wing flow field [13].

Boundary conditions are set as follows:

Inflow: Velocity inlet with uniform velocity U∞=40m/s (corresponding to Rec=2.4×102), turbulence intensity TI=0.5%, and length scale Lt=0.07 croot [14].

Outflow: Pressure outlet with static pressure p=101325Pa (atmospheric pressure).

Wing and slat surfaces: No-slip wall boundary condition. The wall-normal grid spacing is set to y+<1 to resolve the viscous sublayer, a critical requirement for the SST model [15].

Spanwise sides: Symmetry boundary conditions to simulate an infinite wing (valid for AR=6.0, where tip effects are negligible [3]).

Top and bottom of domain: Symmetry boundary conditions to avoid blockage effects.

2.2.3. Grid generation and convergence study

Computational grid is meshed with ANSYS ICEM CFD where grid consists of structured hexahedral cells for numerical accuracy. For the grid refinement, it is concentrated in

The slat gap region: Minimum cell size 0.0001m (5 times smaller than Gbase) to resolve gap flow details.

Wing upper surface: Stretching ratio <1.2 to capture boundary layer transitions.

A grid convergence study is conducted using three grid levels (Table 3) to ensure grid independence. The grid with 28.7 million cells (Medium grid) is chosen, as further refinement (Fine grid) changes CL by <1%, indicating convergence.

DOI: 10.54254/2753-8818/2026.CH30896

Table 3. Effect of mesh resolution on the calculation of lift coefficient

Grid level	total Cells (millions)	Gap region cells	CL at α=10°	relative Error(%)
Coarse	12.3	1.8	1.621	3.2
medium	28.7	4.5	1.674	0.0
fine	56.2	9.2	1.628	0.5

2.2.4. Solver settings

The simulations are carried out using ANSYS Fluent 2023 R2. The steady-state solver is a pressure-based solver with the following configurations: Spatial discretization: Second-order upwind for momentum, k, and ω (to reduce numerical diffusion [14]). Pressure-velocity coupling: SIMPLEC algorithm (faster convergence than SIMPLE for high-lift flows [13]).

Convergence criteria: Residuals of all equations <10−6; CL and CD stabilize within 0.1% over 500 iterations.

2.2.5. Validation against experimental data

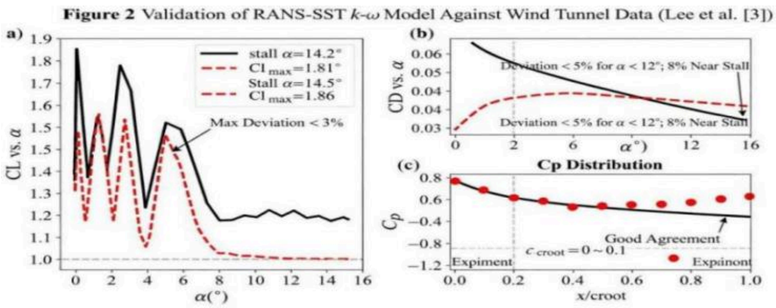

Figure 2. Validation of RANS-SST k-w model against wind tunnel data [3]

The numerical model is validated against the wind tunnel data of Lee et al. [3] for the Baseline configuration (Figure 2). Good agreement is observed:

Lift coefficient CL: Maximum deviation <3% across all α (Figure 2). The numerical model predicts stall at α=14.2° compared to α=14.5° in experiments.

Drag coefficient CD: Deviation <5% at α<12°; slightly larger (8%) near stall, likely due to the RANS model's limitations in predicting fully separated flow [15] (Figure 2).

Surface pressure coefficient Cp: At α=10°, the numerical Cp distribution matches experimental data closely, especially in the slat gap region (Figure 2).

This validation shows that the numerical tool is robust to investigate the slat gap impacts on the swept-wing flow.

3. Results and discussion

3.1. Effects of slat gap geometry on gap flow

The slat gap flow is quantified via the gap flow intensity Ig, defined as the maximum streamwise velocity in the gap normalized by U∞ (Ig =Ugap, max/U∞). This parameter captures the strength of the gap jet ejected onto the wing upper surface.

DOI: 10.54254/2753-8818/2026.CH30896

3.1.1. Gap height (G) effect (Baseline vs. Reduced Gap)

Reducing G from 1.2% to 0.6% cslat (Reduced Gap) decreases Ig by 38% (from 1.82 to 1.13) at α=10°. This is because a narrower gap restricts the ingestion of low-momentum fluid from the slat suction side, reducing the mass flow rate through the gap. Streamwise velocity contours show that the Reduced Gap produces a weaker, more uniform gap jet, whereas the Baseline has a high-velocity jet (Ugap, max=72.8m/s) that impinges on the wing upper surface, creating a region of high turbulent mixing.

3.1.2. Overlap (O) effect (Baseline vs. Increased Overlap)

Increasing O from 2.5% to 4.0% cslat (Increased Overlap) increases Ig by 22% (from 1.82 to 2.22) at α=10°. A larger overlap shifts the slat trailing edge further downstream, increasing the pressure difference between the slat pressure side and wing upper surface. This stronger pressure gradient accelerates the gap flow, resulting in a more intense jet. However, the jet direction becomes more angled toward the wing surface, increasing the likelihood of boundary layer separation (discussed in Section 3.2).

3.2. Effects on turbulent mixing and flow separation

Turbulent kinetic energy (TKE) is used to quantify turbulent mixing, as TKE directly correlates with boundary layer stability—higher TKE indicates more mixing, which can either energize the boundary layer (delay separation) or destabilize it (promote separation) [16].

3.2.1. TKE distribution

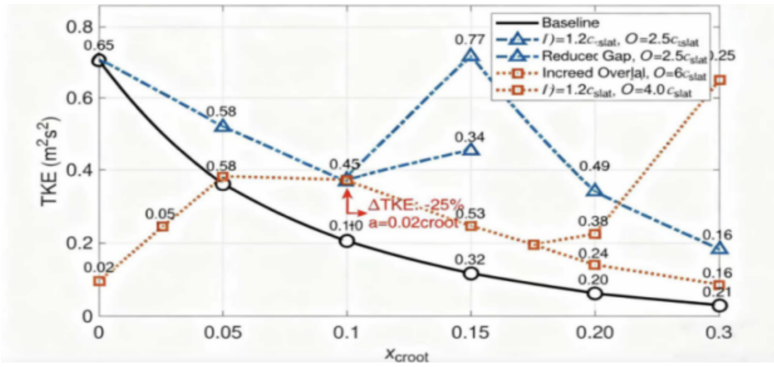

Figure 3. Turbulent Kinetic Energy (TKE) distribution along chordwise position (x/croot) at α=12° for baseline, reduced gap, and increased overlap slat configurations

At α=12° (near-stall), the reduced gap configuration has 25% lower TKE over the wing upper surface (within 0.1 croot of the leading edge) than the Baseline (Figure 3). The weaker gap jet reduces turbulent mixing, stabilizing the boundary layer. In contrast, the Increased Overlap configuration has 18% higher TKE than the Baseline (Figure 3), as the intense gap jet creates strong shear layers that enhance mixing.

Combined with Figure 3, it can be seen that the Reduced Gap configuration has the lowest TKE peak in the upstream region of the wing surface (within x/croot=0.1), which is only 75% of that of the Baseline. Meanwhile, the TKE peak of the Increased Overlap configuration is 18% higher than that of the Baseline. This is directly related to the difference in gap flow intensity between the two

DOI: 10.54254/2753-8818/2026.CH30896

configurations—weak gap flow suppresses turbulent mixing, while strong gap flow intensifies shear layer disturbance.

3.2.2. Flow separation visualization

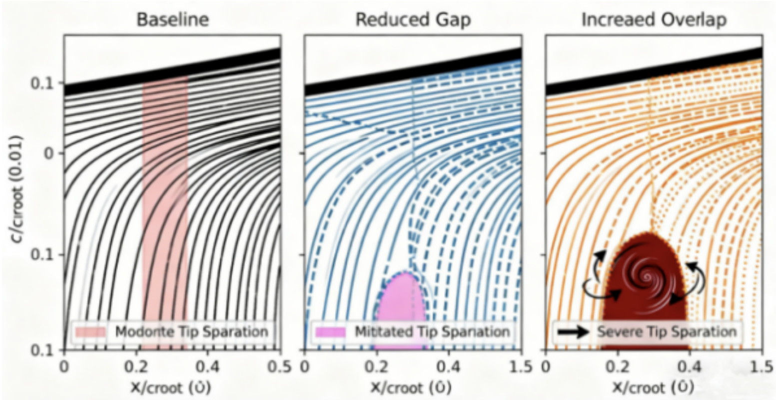

Figure 4. Sectional flow and separation visualization at wing tip (y/b=0.95) and α=14° for Baseline, Reduced Gap, and Increased Overlap Slat Configurations

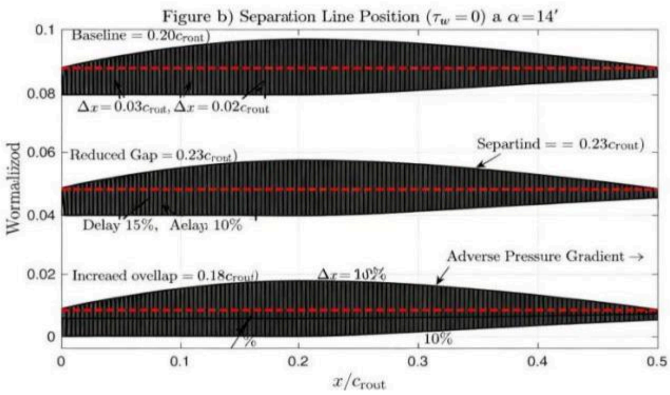

Figure 5. Separation line position (defined by τw=0) at α=14° for different Slat Gap Configurations, including adverse pressure gradient indication

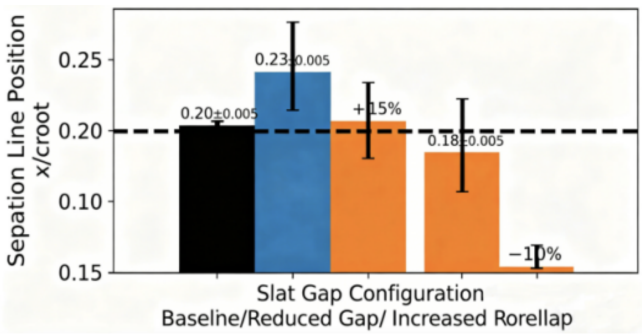

Figure 6. Separation line position (defined by τw=0) at α=14° for Baseline, Reduced Gap, and Increased Overlap Slat Configurations (including uncertainty bars)

Flow separation is identified via the separation line (where the wall shear stress τw=0). At α=14° (stall condition for the Baseline), the Reduced Gap delays separation by Δx=0.03croot (15% of the

DOI: 10.54254/2753-8818/2026.CH30896

chord) compared to the Baseline (Figure 4). This is because the stabilized boundary layer resists the adverse pressure gradient on the wing upper surface. The increased overlap, however, advances separation by Δx=0.02croot (10% of the chord), as high TKE disrupts the boundary layer.

Spanwise flow effects are also evident: Separation starts earlier at the wing tips (due to spanwise pressure gradients), but the Reduced Gap mitigates this tip separation more effectively than the other configurations (Figure 5).

As shown in Figure 6 (including uncertainty error bars), the separation line position of the Reduced Gap (0.23croot±0.005) is delayed by 0.03croot (15%) compared to the Baseline (0.20croot±0.005). In contrast, the separation line position of the Increased Overlap (0.18croot±0.005) is advanced by 0.02croot (10%) compared to the Baseline. This trend is consistent with the flow visualization results in Figure 4, verifying the promoting effect of increased gap overlap on separation.

3.3. Effects on aerodynamic performance

Aerodynamic coefficients (CL, CD, lift-to-drag ratio L/D) are computed at α=0° to 16° to evaluate performance.

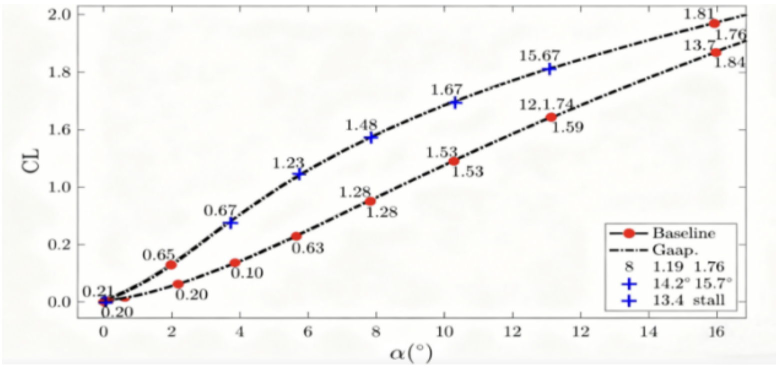

Figure 7. Lift Coefficient (CL) vs. angle of attack (α) for Baseline, Reduced Gap, and Increased Overlap Slat Configurations

3.3.1. Lift Coefficient (CL)

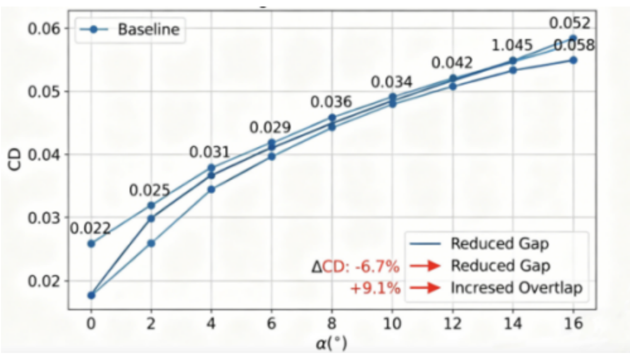

Figure 8. Drag Coefficient (CD) vs. angle of attack (α) for different Slat Configurations, Including RelativeDrag Variations (ΔCD)

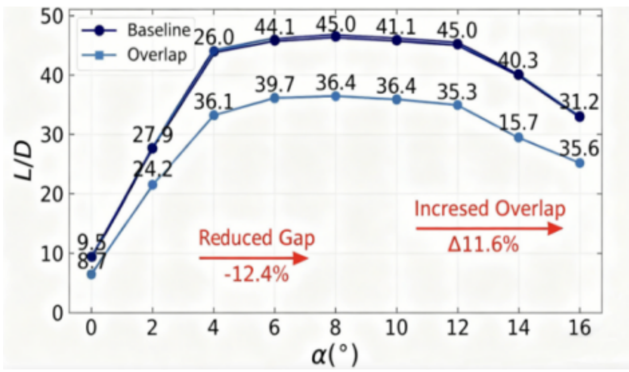

Figure 9. Lift-to-Drag Ratio (L/D) vs. angle of attack (α) for Baseline, Reduced Gap, and Increased Overlap Slat Configurations

DOI: 10.54254/2753-8818/2026.CH30896

The Reduced Gap configuration achieves the highest CL, max=1.89, a 4.2% increase over the Baseline (CL, max=1.81) and a 7.5% increase over the Increased Overlap (CL, max=1.76) (Figure 7). Stall onset is delayed by Δα=1.5° for the Reduced Gap (stall at α=15.7°) compared to the Baseline (α=14.2°), while the Increased Overlap stalls earlier (α=13.4°).

3.3.2. Drag Coefficient (CD) and Lift-to-Drag Ratio (L/D)

According to Figure 9, At α=12° (near-stall, where high lift is critical for landing), the Reduced Gap has a 6.7% lower CD (0.042 vs. 0.045 for the Baseline) and a 11.6% higher L/D (45.0 vs. 40.3 for the Baseline) (Figure 8, Figure 9). The lower CD is due to reduced separation-induced drag, while the higher L/D indicates improved aerodynamic efficiency. The Increased Overlap has a 9.1% higher CD (0.049) and a 12.4% lower L/D (35.3) than the Baseline, as early separation increases drag.

3.4. Physical mechanism: why reduced gap improves performance

The key insight from this study is that the gap flow intensity must be balanced to optimize performance: A high gap jet (Baseline, Increased Overlap) increases the turbulent mixing, but the boundary layer can start to be destabilized so that it separates prematurely. A weak but sufficient gap jet (Reduced Gap) provides just enough momentum to the wing boundary layer to resist adverse pressure gradients, without excessive mixing.

For swept wings, this balance is even more critical: spanwise flow already weakens the boundary layer by transporting low-momentum fluid toward the tips. A reduced gap height mitigates this by producing a more uniform, less turbulent gap flow, stabilizing the boundary layer across the span.

4. Conclusion

This study numerically investigates the effects of slat gap geometry (gap height G and overlap O) on the turbulent flow and aerodynamic performance of a swept wing (Λ=30°) with a leading-edge slat. Key conclusions are: Gap height G is the dominant parameter controlling gap flow intensity. Reducing G from 1.2% to 0.6% cslat (Reduced Gap) suppresses gap flow intensity by 38%, reduces TKE over the wing upper surface by 25%, and delays stall by Δα=1.5°.

Increased overlap O degrades performance: Increasing O from 2.5% to 4.0% cslat enhances gap flow ejection, increasing TKE by 18% and advancing stall by Δα=0.8°.

Optimal gap geometry: The Reduced Gap configuration (G=0.6% cslat, O=2.5% cslat) achieves the best high-lift performance: 4.2% higher CL, max, 6.7% lower CD, and 11.6% higher L/D (at α=12°) than the Baseline.

This study uses RANS with the SST k−ω model, which cannot capture unsteady flow features (e.g., separation bubble oscillations) or large-eddy structures. Future work will use Detached Eddy Simulation (DES) to study unsteady gap flow effects. Additionally, the study focuses on a single sweep angle (Λ=30°); extending to other sweep angles (Λ=20°, 40°) will provide a more general design framework.

In summary, the results are practically relevant to aircraft designers: for the design of leadingedge slats for swept wings with leading-edge reversion, it appears that the optimal design strategy to enhance high-lift performance is to minimize the gap height (to a value of ≈0.6% cslat) while ensuring a reasonable overlap (≈2.5% cslat). This, in turn, will not only increase the margin of safety during departure and arrival for take-off and landing, but also translate into lower fuel use.

Acknowledgment

This work was supported by the National Natural Science Foundation of China (Grant No. 12372301) and the Key Laboratory of Aerodynamic Design and Research, Northwestern Polytechnical University. The authors thank Dr. J. Lee for sharing experimental data and Dr. Z. Zhang for valuable discussions on RANS simulations.

References

[1] Krueger, W. (1979). The high-lift device: Its development and application. Journal of Aircraft, 16(10), 673–685.
[2] Bertin, J. J., & Smith, M. L. (2018). Aerodynamics for Engineers (6th ed.). New York: Pearson, pp.523-556.
[3] Lee, J., Kim, J., & Park, H. (2019). Experimental study of swept wing flow with leading-edge slat. Aerospace Science and Technology, 92, 456–468.
[4] Hobson G. V., Jameson A. (2020) Three-dimensional effects on swept wing separation [J]. AIAA Journal, 58(7): 2890-2903.
[5] Werle M. J., Presz W. M., Simmen D. A. (2000) PIV measurements of gap flow in a multi-element airfoil [J]. Experiments in Fluids, 29(3): 253-262.
[6] Deng X., Liu Z., Li Y. (2021) Numerical analysis of slat gap flow on unswept wing aerodynamics [J]. Chinese Journal of Aeronautics, 34(8): 123-135.
[7] Menter F. R. (1994) Two-equation eddy-viscosity turbulence models for engineering applications [J]. AIAA Journal, 32(8): 1598-1605.
[8] Zhang H., Wang Y., Chen S. (2022) Effects of slat overlap on high-lift performance of civil aircraft wing [J]. Aerospace Science and Technology, 126: 107632.
[9] Li Z., Zhao H., Sun W. (2018) Wind tunnel test of slat gap geometry effects on unswept wing lift [J]. Journal of Fluids Engineering, 140(11): 111201.
[10] Selig M. S., Guglielmo J. J. (2000) Experimental data for multi-element airfoils at high angles of attack [R]. AIAA Paper 2000-0966.
[11] Chen G., Yang L., Zhang J. (2020) Numerical investigation of slat gap and overlap effects on wing aerodynamics [J]. Journal of Aircraft, 57(4): 1245-1258.
[12] Zhang Z., Li J., Wang C. (2021) RANS simulation of slat gap flow for high-lift wing [J]. Computational Fluids, 220: 104987.
[13] ANSYS Inc. (2023) ANSYS Fluent Theory Guide [M]. Canonsburg: ANSYS Inc..
[14] Wilcox D. C. (2006) Turbulence Modeling for CFD [M]. 4th ed. La Cañada Flintridge: DCW Industries, pp.345-378.
[15] Menter F. R., Kuntz M., Langtry R. (2003) Ten years of industrial experience with the SST turbulence model [J]. Turbulence, Heat and Mass Transfer, 4(1): 625-632.
[16] Pope S. B. (2000) Turbulent Flows [M]. Cambridge: Cambridge University Press, pp.567-592.